

Angular-divergence calculation for Experimental Advanced Superconducting Tokamak neutral beam injection ion source based on spectroscopic measurementsa)

Yuan Chi, Chungong Hu, and Ge Zhuang

Citation: [Review of Scientific Instruments](#) **85**, 02A731 (2014); doi: 10.1063/1.4852295

View online: <http://dx.doi.org/10.1063/1.4852295>

View Table of Contents: <http://scitation.aip.org/content/aip/journal/rsi/85/2?ver=pdfcov>

Published by the [AIP Publishing](#)

Articles you may be interested in

[Improvement of a plasma uniformity of the 2nd ion source of KSTAR neutral beam injector](#))

Rev. Sci. Instrum. **85**, 02B316 (2014); 10.1063/1.4830362

[Erratum: "Arc discharge regulation of a megawatt hot cathode bucket ion source for the experimental advanced superconducting tokamak neutral beam injector" \[Rev. Sci. Instrum.83, 013301 \(2012\)\]](#)

Rev. Sci. Instrum. **83**, 129903 (2012); 10.1063/1.4772571

[First plasma of megawatt high current ion source for neutral beam injector of the experimental advanced superconducting tokamak on the test bed](#)

Rev. Sci. Instrum. **82**, 023303 (2011); 10.1063/1.3545843

[Doppler-shift spectra of H \$\alpha\$ lines from negative-ion-based neutral beams for large helical device neutral beam injection](#)

Rev. Sci. Instrum. **77**, 03A538 (2006); 10.1063/1.2166676

[Discharge characteristics of a long pulse ion source for the Korea Superconducting Tokamak Advanced Research neutral beam system](#)

Rev. Sci. Instrum. **71**, 1140 (2000); 10.1063/1.1150409



SHIMADZU Excellence in Science

Powerful, Multi-functional UV-Vis-NIR and FTIR Spectrophotometers

Providing the utmost in sensitivity, accuracy and resolution for a wide array of applications in materials characterization and nanotechnology research

- Photovoltaics
- Polymers
- Thin films
- Paints/inks
- Ceramics
- FPDs
- Coatings
- Semiconductors

[Click here to learn more](#)



Angular-divergence calculation for Experimental Advanced Superconducting Tokamak neutral beam injection ion source based on spectroscopic measurements^{a)}

Yuan Chi,^{1,2,b)} Chundong Hu,² and Ge Zhuang¹

¹State Key Laboratory of Advanced Electromagnetic Engineering and Technology, Huazhong University of Science and Technology, Wuhan 430074, China

²Institute of Plasma Physics, Chinese Academy of Sciences, Hefei 230031, China

(Presented 12 September 2013; received 7 September 2013; accepted 4 November 2013; published online 31 December 2013)

Calorimetric method has been primarily applied for several experimental campaigns to determine the angular divergence of high-current ion source for the neutral beam injection system on the Experimental Advanced Superconducting Tokamak (EAST). A Doppler shift spectroscopy has been developed to provide the secondary measurement of the angular divergence to improve the divergence measurement accuracy and for real-time and non-perturbing measurement. The modified calculation model based on the W7AS neutral beam injectors is adopted to accommodate the slot-type accelerating grids used in the EAST's ion source. Preliminary spectroscopic experimental results are presented comparable to the calorimetrically determined value of theoretical calculation.

© 2013 AIP Publishing LLC. [<http://dx.doi.org/10.1063/1.4852295>]

I. INTRODUCTION

Megawatt high current ion sources¹ for the neutral beam injection (NBI) systems are currently being developed in the Institute of Plasma Physics Chinese Academy of Sciences to provide the auxiliary heating for the Experimental Advanced Superconducting Tokamak (EAST). As one of the key parameters of the beam, the angular divergence should be measured properly in order to optimize the operating conditions of the beam extraction system and to reduce the heat load on beam facing components.^{2,3} Study of transmission and intensity distribution of a heating beam also needs the value of divergence⁴ especially for the case when neutral beam is used for a diagnostic purpose.⁵ The current calorimetric technique in the EAST NBI system suffers from destruction of the measuring devices and is unavailable during beam injection period. Nowadays the use of emission-line with Doppler-shift by the beam particles is widely applied and becomes a standard and non-disturbing tool for neutral beam injectors.⁶⁻⁸ Analysis of the energy fractions as well as the angular divergence can be deduced by the Doppler shift spectroscopy (DSS) measurement.⁹⁻¹¹ For the experiments on the EAST NBI testbed, the intensity of each Doppler-shifted component of H_{α} light is measured and energy fractions are calculated with appropriate cross sections data¹²⁻¹⁴ and analysis model.^{15,16} The angular divergence can be evaluated from the width of each energy component after considering all related broadening effects.

^{a)}Contributed paper, published as part of the Proceedings of the 15th International Conference on Ion Sources, Chiba, Japan, September 2013.

^{b)}Author to whom correspondence should be addressed. Electronic mail: jtext@hust.edu.cn.

II. EXPERIMENTAL SETUP

Figure 1 shows the geometric relationship between the accelerating grid and the arrangement of collecting optics. Four-grid multi-slot accelerator is adopted for the EAST ion source because of high transparency and efficient heat removal performance. Each accelerating grid is fabricated with four identical sub-electrodes. The sub-electrodes in Section I and Section II are inclined to beam direction to focus the beam. Two sub-electrodes in Section ZERO are in the vertical plane with no contributions to beam convergence. Ion beam is extracted along the z-axis through slot apertures, which are parallel to the x-axis. Since the beam cross section is rectangular and the divergence angle is different at each viewing direction, the DSS optical system used on the EAST NBI testbed occupies one viewing port in the vertical plane and two in the horizontal plane. The inclined sightlines respecting to the beam direction to provide the Doppler-shifted measurement have the angle of 46°, 62.5°, and 67.5°. Sightlines of the L_1 lens and L_2 lens intersected the beam axis almost at the same place inside the neutralizer and the L_3 lens viewed the area just behind the exit of the neutralizer. Signals from L_1 , L_2 , and L_3 are relayed to a Czerny-Turner spectrometer using optical fibers. The spectrometer has a focal length of 0.5 m and an aperture of $f/6.5$ equipped with a grating at 1800 groves/mm.

III. CALCULATION MODEL

The broadening effects of beam-emitted light have been thoroughly investigated under the concept of convolution by Bracco *et al.* in Ref. 9. The detailed derivation of formulae and evaluation of experimental results are strongly simplified if the use of $1/e$ widths of the spectrum is taken into account.¹⁷

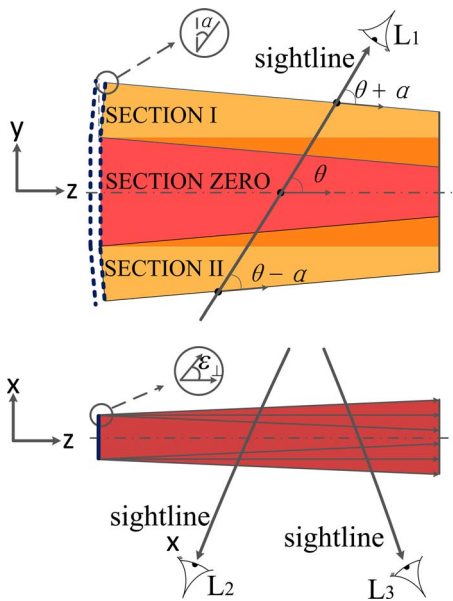


FIG. 1. Geometric relationship between accelerating grids and the arrangement of collecting optics (not drawn to scale). Beam is extracted along z axis. Sightline in the vertical plane (upper picture) integrates light across all three sections. Lenses in the horizontal plane (lower picture) only collect light coming from Section ZERO.

In nonrelativistic approximation the Doppler shift of the H_{α} line at a viewing angle θ with respect to the beam velocity v is given by

$$\Delta\lambda = \lambda_0 \frac{v}{c} \cos \theta, \quad (1)$$

here $\lambda_0 = 6562.8 \text{ \AA}$. The various broadening as a result of a deviation from the central Doppler shift

$$\Delta\lambda_0 = \lambda_0 \frac{v_0}{c} \cos \theta_0 \quad (2)$$

caused by a distribution of v and θ will be

$$\delta \equiv d(\Delta\lambda) = \Delta\lambda_0 \left(\frac{dv}{v_0} + \tan\theta_0 d\theta \right). \quad (3)$$

A. Ion source temperature

The ion source has a finite temperature of the order of a few eV. The angular divergence caused by perpendicular beam temperature of the beam with energy E_{beam} is

$$\varepsilon_{\perp} = \sqrt{\frac{T_{\perp}}{E_{\text{beam}}}}, \quad (4)$$

and the Gaussian 1/e half-width of the spectral line only considering T_{\perp} is

$$\delta_{\perp} = \varepsilon_{\perp} \Delta\lambda_0 \tan \theta_0. \quad (5)$$

Parallel beam temperature contributing to the 1/e half-width of the spectral line is

$$\delta_{\parallel} = \varepsilon_{\parallel} \Delta\lambda_0. \quad (6)$$

Beam parallel energy spread is strongly compressed by the parallel acceleration.¹⁷ The high-voltage ripple is not considered for the same reason.

B. Sightline cross-section

The cross-section of sightline also blows up the measured linewidth. Additional divergence can be obtained by the fiber diameter, the focal length of the collecting lens. Sometimes the viewing port may act as an aperture stop. Similar to Eq. (5) the Gaussian 1/e linewidth caused by light collecting system is

$$\delta_{L_i} = \varepsilon_{L_i} \Delta\lambda_0 \tan \theta_0, \quad i = 1 - 3, \quad (7)$$

where ε_{L_i} is calculated from the geometric-optical relation for each lens.

C. Instrument broadening

Since a spectrometer is used to analysis the beam emitted H_{α} lines, instrumental broadening δ_{instr} is monitored routinely during experiments.

D. Beam focusing

Beam focusing also makes a contribution to the line broadening for a spherical shape accelerating grid but this is not the case for the EAST ion source. Ions are not focused in the x direction and partially focused in the y direction by the sub-electrodes in Section I and Section II. A summation of three Gaussian functions as Eq. (8) is used as the target function in the fitting procedure for each energy peak for the spectra collected from L_1 . The fitting function is

$$y_{\text{fit}} = A \exp\left(-\frac{(\lambda - \lambda_1)^2}{2\sigma^2}\right) + A \exp\left(-\frac{(\lambda - \lambda_2)^2}{2\sigma^2}\right) + 2A \exp\left(-\frac{(\lambda - \lambda_0)^2}{2\sigma^2}\right), \quad (8)$$

where λ_1 and λ_2 are Doppler-shifted wavelengths caused by the small inclined angles ($\alpha = 1.083^\circ$) of sub-electrodes in Section I and Section II. Three sub-components in Eq. (8) represent the beam emitted light from the three sections, respectively. The light integration length in Section ZERO is twice as that in Section I and Section II; therefore, the magnitude of the third part is two times larger than the first two in Eq. (7). As light comes from all sections bearing the same broadening effect, the width control σ in each part has the same value in Eq. (8).

Considering all the broadening effects discussed above the total 1/e width of spectral line becomes

$$\delta_{L_i} = \sqrt{\delta_{\perp}^2 + \delta_{\parallel}^2 + \delta_{L_i}^2 + \delta_{\text{instr}}^2}, \quad i = 1 - 3. \quad (9)$$

Then the influences of parallel and perpendicular beam temperature can be derived using Eq. (9) for three independent spectral results from collecting lenses which have different angles inclined to the beam.

Angular beam divergence in the x and y directions can be derived from Eq. (9) using spectra from L_2 , L_3 , and L_1 :

$$\varepsilon_{x,i} = \sqrt{\frac{\delta_{L_i}^2 - \delta_{\text{instr}}^2}{(\Delta\lambda_0 \tan \theta_i)^2} - \varepsilon_{L_i}^2}, \quad i = 2, 3, \quad (10)$$

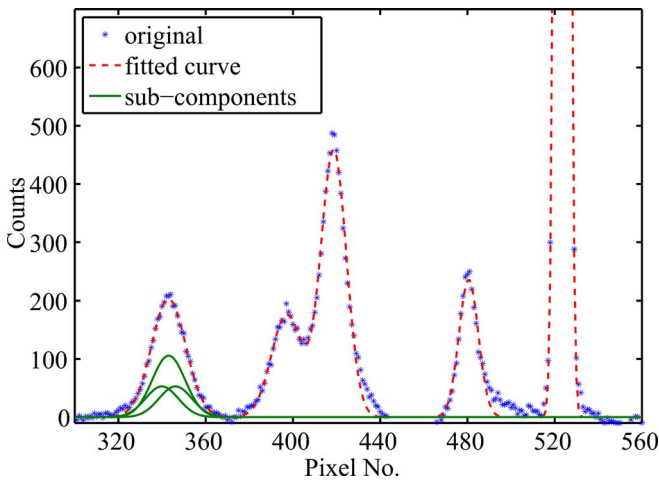


FIG. 2. A typical spectrum observed by L_1 including sub-components for fitting. Solid lines show the sub components of the full energy peak.

$$\varepsilon_{y,i} = \sqrt{\frac{\delta_{L_1}^2 - \delta_{instr}^2}{(\Delta\lambda_0 \tan \theta_i)^2} - \varepsilon_{L_i}^2 - \alpha}, \quad i = 1. \quad (11)$$

A spectrum of H_α lines emitted by a typical shot observed by L_1 with preliminary results is shown in Figure 2. In the blue shifted spectrum each energy peak is fitted by using Eq. (8) and the sub-components of the full energy peak are plotted.

IV. RESULTS

Based on the model given in Ref. 3 calorimetric determined beam divergence at any operation range in theoretical calculation can be drawn as a reference line which is mainly related to the geometry of accelerating grids. During the experiments on the EAST NBI testbed we tried to find well coupled operation parameters to make a good beam fo-

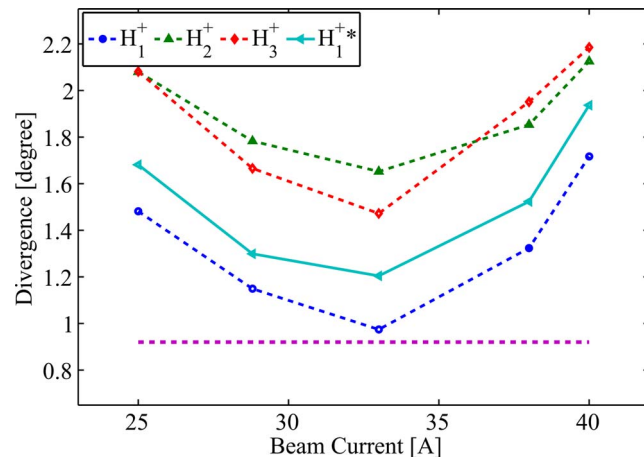


FIG. 3. Beam divergence as a function of extraction current at a fixed accelerating voltage (52 kV). The solid line shows the single Gaussian fitting results for the full energy component. Calorimetrically determined results of theoretical calculation are also presented (straight line).

cus performance. Beam divergence as a function of extraction current at a fixed accelerating voltage is shown in Figure 3. The results are calculated from the spectra collected from L_1 . Equation (8) is used for curve fitting. Meanwhile the full energy component is also fitted with single Gaussian function for comparison. It can be seen that the former fitting result at the best match operation point around 33 A is closer to the calorimetrically reference line. The remained gap may result from the uncertain sightline cross section which is difficult to determine after beamline assembly.

V. CONCLUSIONS

Preliminary spectroscopic determined beam angular divergence of each energy component was presented. The DSS on the EAST NBI testbed is proved to be an important additional diagnostic tool for beam divergence measurement to optimize EAST NBI operation range. The influence of the sightline cross section need to be checked in the future experiment.

ACKNOWLEDGMENTS

We would like to thank all EAST NBI group members for the helps in this work.

- ¹C. D. Hu and Y. H. Xie, *Plasma Sci. Technol.* **14**(1), 75 (2012).
- ²C. F. Burrell, W. S. Cooper, R. R. Smith, and W. F. Steele, *Rev. Sci. Instrum.* **51**(11), 1451–1462 (1980).
- ³Y. J. Xu and C. D. Hu, *Sci. China Phys. Mech. Astron.* **54**(2), 300–304 (2011).
- ⁴J. Kim and J. H. Whealton, *Nucl. Instrum. Methods* **141**(2), 187–191 (1977).
- ⁵M. Sasao, K. Connor, K. Ida, H. Iguchi, A. Ivanov, M. Nishiura, D. Thomas, M. Wada, and M. Yoshinuma, *IEEE Trans. Plasma Sci.* **33**(6), 1872–1900 (2005).
- ⁶K. H. Berkner, C. F. Chan, W. S. Cooper, R. R. Smith, W. F. Steele, and J. W. Stearns, *Bull. Am. Phys. Soc.* **23**(7), 913–913 (1978).
- ⁷J. H. Kamperschroer, H. W. Kugel, M. A. Reale, S. L. Hayes, G. A. Johnson, J. L. Lowrance, P. A. Shah, P. Sichta, B. W. Sleford, M. D. Williams, and P. M. Zucchini, *Rev. Sci. Instrum.* **58**(8), 1362–1368 (1987).
- ⁸J. H. Kamperschroer, L. R. Grisham, N. Kokatnur, L. J. Lagin, R. A. Newman, T. E. O'Connor, T. N. Stevenson, and A. v. Halle, *Rev. Sci. Instrum.* **66**(1), 130–138 (1995).
- ⁹G. Bracco, C. Breton, C. d. Michelis, M. Mattioli, and J. Ramette, *J. Opt. Soc. Am.* **71**(11), 1318–1326 (1981).
- ¹⁰S. J. Yoo, H. L. Yang, and S. M. Hwang, *Rev. Sci. Instrum.* **71**(3), 1421–1424 (2000).
- ¹¹J. Fu, Y. J. Shi, Y. Y. Li, F. D. Wang, S. Liu, J. Zhang, J. Li, Y. Y. Huang, Y. L. Xie, and Z. M. Liu, *J. Korean Phys. Soc.* **58**(5), 1141–1145 (2011).
- ¹²J. Kim and H. H. Haselton, *J. Appl. Phys.* **50**(6), 3802–3807 (1979).
- ¹³I. D. Williams, J. Geddes, and H. B. Gilbody, *J. Phys. B* **15**(9), 1377–1389 (1982).
- ¹⁴I. D. Williams, J. Geddes, and H. B. Gilbody, *J. Phys. B* **16**(24), L765 (1983).
- ¹⁵R. Uhlemann, R. S. Hemsworth, G. Wang, and H. Euringer, *Rev. Sci. Instrum.* **64**(4), 974–982 (1993).
- ¹⁶E. Delabie, M. Brix, C. Giroud, R. J. E. Jaspers, O. Marchuk, M. G. O'Mullane, Y. Ralchenko, E. Surrey, M. G. von Hellermann, K. D. Zastrow, and JET-EFDA Contributors, *Plasma Phys. Controlled Fusion* **52**(12), 125008 (2010).
- ¹⁷W. Ott and F. P. Penningsfeld, Tech. Rep. IPP 4/258 (1993).